Amyloid Formation Modulates the Biological Activity of a Bacterial Protein*

Sylvain Bieler‡§, Lisbell Estrada‡, Rosalba Lagos¶, Marcelo Baeza¶, Joaquín Castilla‡, and Claudio Soto‡¶‖

From the ‡Department of Neurology, University of Texas Medical Branch, Galveston, Texas 77555 , §Department of Cell Biology, University of Geneva, CH-1211 Geneva 4, Switzerland, and ¶Departamento de Biología, Universidad de Chile, Casilla 653, Santiago, Chile

The aggregation of proteins into amyloid fibrils is the hallmark feature of a group of late-onset degenerative diseases including Alzheimer, Parkinson, and prion diseases. We report here that microcin E492, a peptide naturally produced by *Klebsiella pneumoniae* that kills bacteria by forming pores in the cytoplasmic membrane, assembles *in vitro* into amyloid-like fibrils. The fibrils have the same structural, morphological, tinctorial, and biochemical properties as the aggregates observed in the disease conditions. In addition, we found that amyloid formation also occurs *in vivo* where it is associated with a loss of toxicity of the protein. The finding that microcin E492 naturally exists both as functional toxic pores and as harmless fibrils suggests that protein aggregation into amyloid fibrils is an evolutionarily conserved property of proteins that can be successfully employed by bacteria to fulfill specific physiological needs.

Bacteriocins form a vast and diverse group of antibacterial proteins that have been found in most lineages of Eubacteria and Archaebacteria. They kill or inhibit the growth of closely related species by binding to specific cell surface receptors and by forming ion channels in the cytoplasmic membrane, degrading DNA, blocking protein translation, or inhibiting peptidoglycan synthesis (1). They have been proposed to be involved in maintaining bacterial diversity by mediating interactions at the population and community levels (2).

Microcin E492 (Mcc)[1] is a low molecular weight bacteriocin naturally produced by *Klebsiella pneumoniae* RYC492 that is active against several strains of Enterobacteriaceae (3–5). Its mechanism of action has been shown to involve the formation of pores in the cytoplasmic membrane of target cells and subsequent lethal loss of membrane potential (5–7). Whereas most known microcins are only produced when exponential growth ceases and the cells enter the stationary phase (8), Mcc activity has been reported to be highest during the exponential phase and to suddenly drop to virtually undetectable levels during the stationary phase (3, 9). Surprisingly, Mcc was found to be similarly produced and accumulated both in exponential and stationary phases (10), thereby ruling out an arrest of Mcc production and/or degradation as causes of this loss of activity. In addition, mass spectrometry studies revealed no difference in the molecular weight of Mcc purified from either growth phases, indicating that this effect was not related to any post-translational modifications of the protein under our experimental conditions.[2] This led us to hypothesize that the sudden disappearance of activity in the stationary phase could be because of a change in Mcc conformation and/or oligomerization state.

We report here that purified active Mcc is able to be converted upon *in vitro* incubation from a soluble to an insoluble state consisting of amyloid-like fibrils. Electron microscopy, structural, biochemical, and kinetics studies indicate that these fibrils have properties identical to those previously described for the amyloid aggregates that are formed in the course of amyloid diseases. We also found that the assembly of Mcc into amyloid fibrils is accompanied by a loss of the antibacterial activity of the protein. Furthermore, amyloid fibrils are also formed *in vivo*, and this correlates with a sudden drop in Mcc activity in the culture. We therefore propose that amyloid formation modulates the activity of Mcc *in vivo* and is responsible for the previously reported loss of activity in the stationary phase. These data represent the first demonstration that amyloid formation in prokaryotes controls *in vivo* the biological activity of a protein and changes the phenotype of the bacteria. Thus far, formation of amyloid has been associated with several human diseases involving the misfolding, aggregation, and tissue deposition of proteins (11–13). Our findings suggest that the process of protein aggregation into amyloid fibrils is a conserved mechanism that may have an important role not only in triggering tissue damage and disease but also in modulating the biological activity of diverse proteins.

EXPERIMENTAL PROCEDURES

Bacterial Strains and Plasmids—The *Escherichia coli* strains and plasmids used in this study are described in Table I.

Growth Conditions—Bacteria were grown at 37 °C with shaking in LB (Luria-Bertani) Miller medium (14) that was filtered through a 0.22-μm cellulose acetate filter system (Corning). When specified, the medium was buffered with 100 mM PIPES-NaOH at pH 6.5. Antibiotics were used at the following concentrations: ampicillin, 100 μg/ml; kanamycin, 50 μg/ml. Cultures were started using 1:1000 dilutions of fresh overnight cultures to minimize the amount of amyloid-like Mcc from the inocula.

Purification of Mcc—E. coli VCS257pJEM15 was grown at 37 °C with shaking to an absorbance at 600 nm of 1.5 in M9 minimal medium containing 0.2% glucose, 0.2% sodium citrate, 1 g/liter casamino acids, 1 mg/liter thiamine, and 100 mg/liter ampicillin. 200 ml of culture supernatant were passed through a Sep-Pak C18 cartridge (Waters). The cartridge was washed with 3 ml of 65% methanol and 3 ml of 25%

* This work was supported in part by Grants FONDECYT 1020757 and 7020757 and National Institutes of Health Grants AG0224642 and NS549173. The costs of publication of this article were defrayed in part by the payment of page charges. This article must therefore be hereby marked "*advertisement*" in accordance with 18 U.S.C. Section 1734 solely to indicate this fact.

‖ To whom correspondence should be addressed. Tel.: 409-747-0017; Fax: 409-747-0020; E-mail: clsoto@utmb.edu.

[1] The abbreviations used are: Mcc, microcin E492; LB, Luria-Bertani; PIPES, 1,4-piperazinediethanesulfonic acid; CR, Congo red; ThT, thioflavin T; PK, proteinase K.

[2] S. Bieler, R. Lagos, and C. Soto, unpublished data.

TABLE I
Bacterial strains and plasmids

Strain/plasmid	Genotype	Source or reference
E. coli strains		
VCS257	DP50 *supF* [*supE*44 *supF*58 *hsdS*3(r_{B^-} m_{B^-}) *dapD*8 *lacY*1 *glnV*44 Δ(*gal-uvrB*)47 *tyrT*58 *gyrA*29 *tonA*53 Δ(*thyA*57)]	Stratagene
BL21	F^- *ompT hsdS*(r_{B^-}, m_{B^-}) *gal dcm*	Amersham Biosciences
BL21(DE3)	BL21 λ(DE3)	Novagen
Plasmids		
pJEM15	Mcc determinants	28
np108	Mcc determinants *mceG*::Tn*5*	27
p11α2	Amp^r, fragment of tubulin cloned in pT7–7	28

acetonitrile. Mcc was eluted with 3 ml of 50% acetonitrile and concentrated by a CentriVap Concentrator (Labconco). Samples were brought to pH 8.0 by adding NaOH and incubated at 37 °C for 15 min to ensure full solubilization of aggregates formed during the concentration step. Finally, samples were centrifuged at 75,000 × *g* for 1 h at 4 °C to remove any remaining aggregates, and supernatants were stored at −20 °C. Purity was calculated to be >90% by amino acid composition analysis (420/H Amino Acid Analysis System; Applied Biosystems). Matrix-assisted laser desorption ionization time-of-flight mass spectrometry performed in a Voyager DE STR biospectrometry work station (Applied Biosystems) revealed one single peak at 7887.5 Da corresponding to the previously reported molecular mass of mature Mcc without post-translational modifications (5, 15).

Electron Microscopy—Samples of purified Mcc or bacterial culture were placed onto 300-square mesh nickel grids (Maxtaform), negatively stained with 2% uranyl acetate for 90 s, and examined in a Philips EM410 electron microscope.

Circular Dichroism Analysis—CD spectra were obtained using an AVIV CD spectrometer model 215 with a 0.1-cm path length cell. Five consecutive readings at 1-nm bandwidth, 0.25-s response time, and 1-nm resolution were taken over the wavelength range 190–260 nm at 25 °C, averaged, buffer subtracted, and noise reduced. Mean residue molar ellipticities of Mcc were calculated using 7886.5 as molecular weight and 84 as the number of residues. Samples were sonicated prior to analysis to ensure homogeneity.

Congo Red Binding—For spectral analysis, aggregated Mcc was obtained by incubating the protein at 750 μg/ml in aggregation buffer (10 mM PIPES-NaOH, pH 6.5, 0.5 M NaCl) at 37 °C with agitation for 15 h. Samples were briefly sonicated and incubated with 12.5 μM Congo red (CR) (Aldrich) for 15 min at 37 °C. Absorbance was measured from 400 to 700 nm with a resolution of 1 nm using a DU 530 spectrophotometer (Beckman Coulter). The spectrum of bound CR was obtained by subtracting the spectrum of Mcc alone from the spectrum of Mcc in the presence of CR. The spectrum of free CR was obtained by subtracting the spectrum of the buffer from the spectrum of CR in buffer in the absence of Mcc.

To quantitate amyloid formation by CR assay, Mcc samples (200 μg/ml) were incubated with 44 μM CR for 15 min at 37 °C and centrifuged at 16,000 × *g* for 5 min at room temperature. The absorbance of supernatants was recorded at 490 nm using an EL800 Universal Microplate Reader (Bio-Tek Instruments). The percentage of free CR was obtained by comparison with the absorbance of a sample devoid of protein.

Thioflavin T Fluorescence—For spectral analysis, aggregated Mcc was briefly sonicated, diluted in the aggregation buffer to a final concentration of 3 μM and added 5 μM thioflavin T (ThT) (Aldrich). After 10 min of incubation at room temperature, fluorescence measurements were carried out on a Fluorolog 2 spectrofluorimeter (Spex Industries). The excitation wavelength was set at 430 nm, emission wavelengths ranged from 440 to 700 nm, and slit widths were 6 mm for excitation and emission.

To quantitate amyloid formation by ThT assay, fluorescence emission was measured in the presence of ThT at 480 nm. The excitation wavelength was set at 430 nm, and slit widths were 6 mm for excitation and emission. Fluorescence emission is expressed as arbitrary units.

Proteinase K Digestion—Samples were incubated for 20 min at 37 °C under agitation with the indicated concentrations of proteinase K (PK) (Roche Applied Science). The reaction was stopped by boiling the samples at 102 °C for 5 min in NuPAGE LDS sample buffer (Invitrogen). To assess the resistance of soluble and aggregated Mcc to increasing concentrations of PK, purified Mcc was diluted at 15 μg/ml in culture medium (LB medium, 100 mM PIPES-NaOH, pH 6.5) and either directly digested (soluble) or incubated for 15 h at 37 °C with agitation prior to digestion (aggregated).

Turbidity Assay—Mcc was diluted in aggregation buffer at a final concentration of 850 μg/ml and incubated at 37 °C with agitation. The aggregation of the protein was monitored by measuring the absorbance at 562 nm using a BioPhotometer 6131 (Eppendorf).

Sedimentation Assay and Seeding of Mcc Aggregation—Samples of Mcc at 150 μg/ml in aggregation buffer were incubated at 37 °C with agitation for the indicated times and centrifuged at 16,000 × *g* for 5 min at room temperature. Protein concentration in supernatants was measured using a Micro BCA protein assay kit (Pierce). The amount of aggregated protein was obtained by subtracting this value from the total concentration of Mcc. Aggregated Mcc used to seed aggregation was obtained by incubating the protein at 150 μg/ml in aggregation buffer at 37 °C with agitation for 15 h. Sonicated aggregated Mcc was obtained by submitting the aggregated protein to sonication three times for 3 s at 60% power using a Vibra-Cell ultrasonic processor (Sonics & Materials).

Mcc Activity Assay by the Critical Dilution Method—Samples to be tested were serially diluted in 50% methanol. In the case of cultures, cells were previously removed by centrifugation at 16,000 × *g* for 5 min at room temperature. 4-μl drops of diluted samples were laid onto LB agar plates previously covered with 3 ml of LB top agar containing 2×10^7 Mcc-sensitive *E. coli* BL21(DE3)p11α2 cells. After 15 h of incubation at 37 °C the activity was determined by the critical dilution method and expressed in arbitrary units/ml (16).

Mcc Activity Assay by Counting Surviving Cells—90 μl of samples to be tested were added to 10 μl of *E. coli* BL21(DE3)p11α2 cells grown overnight in LB medium. After 30 min of incubation at 37 °C with shaking, surviving cells were counted by plating serial dilutions onto LB agar. The activity was expressed as a percentage, taking as a reference (100%) the killing activity obtained using a Mcc sample that was not incubated.

Immunoblotting—Samples were diluted in sample buffer (Invitrogen), boiled at 102 °C for 5 min, and loaded on NuPAGE 4–12% bis-Tris gels (Invitrogen). Proteins were transferred to Hybond-ECL nitrocellulose membranes (Amersham Biosciences), incubated with a rabbit antiserum raised against a C-terminal fragment of Mcc (SGSGYNSATSSSGSGS) (1:3000), washed, incubated with a horseradish peroxidase-linked anti-rabbit donkey antibody (1:5,000; Amersham Biosciences), and developed with ECL plus (Amersham Biosciences).

RESULTS

Soluble Mcc Assembles into Amyloid-like Fibrils in Vitro—Negative stain electron microscopy of samples of soluble purified Mcc incubated in LB medium, 100 mM PIPES, pH 6.5 (culture medium) for 15 h at 37 °C revealed ~10-nm-wide unbranched amyloid-like fibrils of varying lengths (Fig. 1, *A* and *B*), whereas no fibrils could be detected in samples of the purified protein that had not been incubated (Fig. 1*C*). Fibrils undistinguishable from those obtained in culture medium were observed upon incubation in 100 mM PIPES-NaOH, pH 6.5, 0.5 M NaCl (Fig. 1*D*).

Circular dichroism studies indicated that whereas soluble Mcc adopts a random coil conformation in aqueous buffer (Fig. 2*A*, *solid line*) or a mainly α-helical one in methanol (Fig. 2*B*, *solid line*), aggregated Mcc is rich in β-sheet structures in both solvents (Fig. 2, *A* and *B*, *dashed lines*). These results are consistent with the stable cross-β-sheet structure that has been proposed for amyloid fibrils (17). A similar structural conversion from a soluble α-helical/random coil conformation into

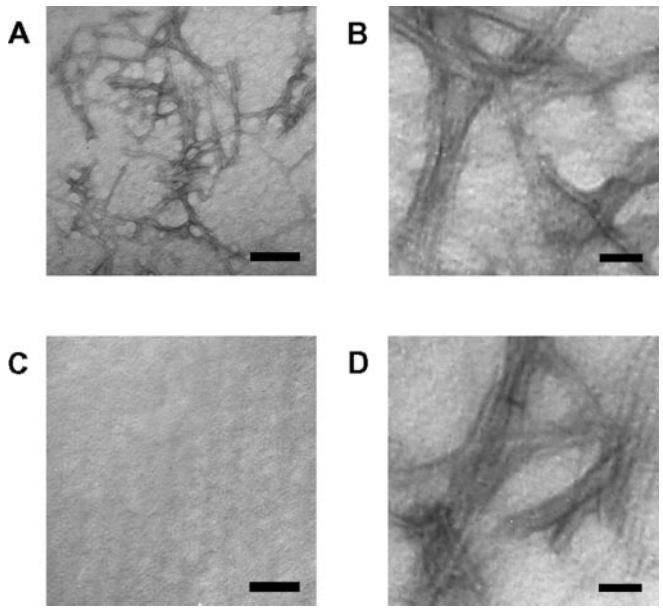

FIG. 1. **Electron micrographs of negatively stained Mcc.** Samples of purified Mcc at 200 μg/ml in culture medium were incubated for 15 h at 37 °C with agitation and examined using a magnification of ×15,000 (*A*) and ×40,000 (*B*). *C*, sample identical to those used in *panels A* and *B* but without incubation, examined using a magnification of ×15,000. *D*, purified Mcc diluted at 200 μg/ml in 100 mM PIPES-NaOH, pH 6.5, 0.5 M NaCl, incubated for 15 h at 37 °C with agitation, and examined using a magnification of ×40,000. *Bars*, 200 nm (*A* and *C*) and 50 nm (*B* and *D*).

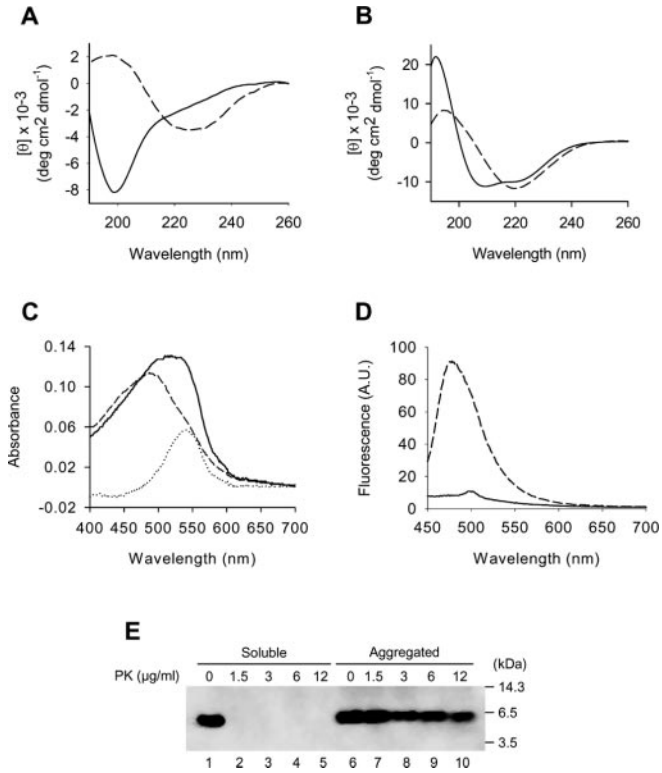

FIG. 2. **Amyloid properties of Mcc assessed by circular dichroism, Congo red binding, thioflavin T binding, and proteinase K digestion.** *A* and *B*, circular dichroism spectra of fresh soluble Mcc (*solid line*) or aggregated Mcc after 15 h of incubation at 37 °C with agitation (*dashed line*). Samples of 1.4 mg/ml Mcc were incubated in 100 mM PIPES-NaOH, pH 6.5, 0.5 M NaCl for 0 or 15 h and diluted 1:10 in 10 mM sodium acetate, pH 4.0 (*A*) or in 100% methanol (*B*) prior to analysis. *C*, absorbance spectra of CR bound to aggregated Mcc (*solid line*), free CR (*dashed line*), and difference between the two spectra (*dotted line*). *D*, fluorescence spectra of ThT alone (*solid line*) and of ThT in the presence of aggregated Mcc (*dashed line*). *A.U.*, arbitrary units. *E*, Mcc immunoblot of PK-treated samples of soluble (*lanes 1–5*) and aggregated (*lanes 6–10*) Mcc. *Lanes 1* and *6*, no PK. *Lanes 2–5* and *7–10*, increasing concentrations of PK (1.5–12 μg/ml). Note that Mcc always appears as a monomer regardless of its aggregation state because of sample preparation for SDS-PAGE (see "Experimental Procedures").

β-sheet-rich aggregates is the hallmark and likely the triggering event in protein misfolding diseases (11, 18).

A typical feature of amyloid fibrils that is used to differentiate them from other types of aggregates is the specific binding and staining with dyes such as CR and ThT (19, 20). Like previously described amyloids (21), aggregated Mcc induced a spectral change in the absorbance of CR with a maximum difference between free CR and Mcc-bound CR at ~540 nm (Fig. 2*C*). The addition of aggregated Mcc to a solution of ThT resulted in a fluorescence emission maximum at ~480 nm (Fig. 2*D*), which is identical to the fluorescence induced by other amyloid proteins (22). Another typical feature of amyloid aggregates is their high resistance to proteolytic degradation, which is partly the reason for the difficulty in clearing them from the body in the disease condition (23, 24). Although soluble Mcc was totally digested by low concentrations of PK, aggregated Mcc exhibited strong resistance to this enzyme at various concentrations (Fig. 2*E*).

CR binding, ThT fluorescence, and protein sedimentation were employed to monitor amyloid formation by Mcc over time as described under "Experimental Procedures." The curves obtained (Fig. 3, *A–C*, *solid line*) are reminiscent of previously described amyloid formation kinetics (25). Indeed, a lag phase where virtually no amyloid-like structures could be detected was followed by a sudden and fast increase in CR binding, ThT fluorescence, or protein precipitation. Similar kinetics was observed when Mcc aggregation was followed by measuring the increase in turbidity of the solution (data not shown). The time course aggregation data suggest that Mcc, similarly to other amyloid proteins, assembles into fibrils following a typical nucleation-dependent polymerization process. This involves a slow nucleation phase in which the unassembled polypeptides undergo unfavorable association steps to form an ordered oligomeric nucleus that is required to initiate rapid polymerization (25). Such a model implies that the lag phase could be bypassed by adding preformed nuclei or seeds. To test this hypothesis, soluble Mcc was incubated in the presence of previously aggregated Mcc, and protein aggregation was followed by sedimentation. As expected, the lag phase was significantly shortened (Fig. 3*C*, *dashed line*) by comparison with the incubation of the soluble protein alone (Fig. 3*C*, *solid line*). Because these seeds consisted of mature fibrils that are presumably not as efficient seeds as small oligomeric nuclei, a similar experiment was performed using sonicated fibrils instead of intact ones. Addition of sonicated fibrils resulted in a complete elimination of the lag phase (Fig. 3*C*, *dotted line*), indicating that sonication was efficient in breaking the fibrils and multiplying the number of seeds available for polymerization, as we described previously for the conversion of the prion protein (26). In addition, this nucleation-dependent amyloid formation model implies that the concentration of soluble Mcc needs to be over a threshold level referred to as critical concentration to initiate polymerization. This critical concentration also corresponds to the concentration of protein that remains in solution when amyloid formation is complete and the system is at equilibrium (25). Fig. 3*C* shows that only ~110 μg/ml Mcc can be aggregated from a total of 150 μg/ml incubated protein, which means that under these conditions the critical concentration is ~40 μg/ml or 5 μM. After this critical concentration is reached, a certain lag time is needed for protein-protein

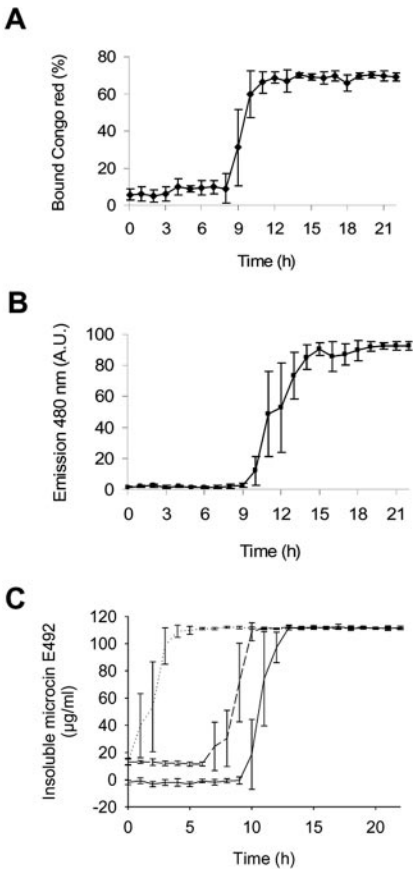

FIG. 3. **Kinetics of Mcc aggregation.** *A*, Mcc aggregation was monitored by measuring the amount of CR bound to the amyloid aggregates as described under "Experimental Procedures." For each time point, three independent Mcc samples were used. *Error bars* indicate S.D. *B*, ThT fluorescence in the presence of Mcc previously allowed to aggregate for the indicated times. For each time point, three independent samples were tested. *Error bars* indicate S.D. *A.U.*, arbitrary units. *C*, seeding of Mcc aggregation. Evolution over time of the amount of aggregated Mcc measured by sedimentation following incubation of soluble Mcc at 150 μg/ml in the absence of previously aggregated Mcc (*solid line*), in the presence of 10% previously aggregated Mcc (*dashed line*), or in the presence of 10% previously aggregated protein subjected to sonication (*dotted line*). For each time point, three independent Mcc samples were used. *Error bars* indicate S.D.

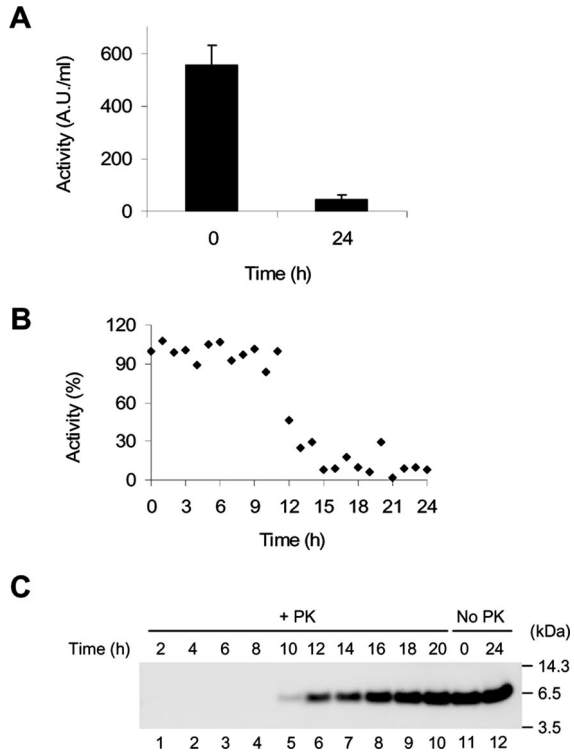

FIG. 4. **Relationship between Mcc activity and aggregation.** Samples of purified Mcc (200 μg/ml) were incubated at 37 °C with agitation in culture medium. *A*, activity of Mcc measured by the critical dilution method either immediately or after 24 h of incubation. For either time point, three independent Mcc samples were used. *Error bars* indicate S.D. *B*, evolution of the activity of Mcc over time measured by counting the number of surviving sensitive cells following exposure to samples of Mcc incubated for the indicated times. The activity is expressed as a percentage, taking as a reference (100%) the killing activity obtained using a Mcc sample that was not incubated. *C*, immunoblot of Mcc samples incubated for the indicated times and subsequently digested (*lanes 1–10*) or not (*lanes 11* and *12*) with PK (3 μg/ml) as described under "Experimental Procedures." The samples used were the same as in *panel B*.

interaction to occur, enabling the formation of a nucleus that further sustains protein polymerization.

In Vitro Polymerization of Mcc into Amyloid Fibrils Is Accompanied by a Loss of Activity—The relation between Mcc activity and amyloid formation was investigated by following over time the ability of soluble or aggregated Mcc to kill sensitive cells. The activity of Mcc before and after 24 h of incubation was measured by the critical dilution method, which revealed a loss of more than 90% of the activity upon aggregation (Fig. 4*A*). In addition, the activity was monitored by counting the number of surviving cells after exposure to Mcc aliquots incubated for various times. The results show that the activity was high during a period of 10 h, which was followed by a sudden and fast loss of activity (Fig. 4*B*). The kinetics of the change in activity mirrored closely the kinetics of amyloid formation as shown in Fig. 3, suggesting that the loss of activity was related to protein aggregation. To rule out the possibility that the loss of cytotoxic activity was because of protein degradation, we compared the amount of protein before and after 24 h of incubation. As shown in Fig. 4*C*, *lanes 11* and *12*, no difference was observed in the total amount of Mcc before and after incubation. The evolution of the PK resistance of Mcc upon incubation was also assessed. Mcc remained fully sensitive to PK for almost 10 h and then became increasingly resistant to this enzyme (Fig. 4*C*), which correlates with the loss of activity (Fig. 4*B*). As shown in Fig. 2, formation of amyloid is paralleled by acquisition of protease resistance; therefore, we conclude from these experiments that Mcc loses its toxic activity upon fibrillar aggregation.

The Loss of Mcc Activity in Vivo Coincides with Amyloid Formation—A culture of Mcc-producing bacteria (*E. coli* BL21pJEM15) was monitored by periodically measuring its optical density at 600 nm and the Mcc activity present in the medium (Fig. 5*A*). The activity was found to accumulate during growth to reach its highest level at the end of the exponential phase of growth (9 h) and then to dramatically drop (10 h) and remain at virtually undetectable levels during the stationary phase. This phenomenon is not restricted to our experimental conditions involving a recombinant *E. coli* strain. Indeed, an identical pattern of activity was previously reported in the original *K. pneumoniae* RYC492 strain, where both active and inactive forms of Mcc were observed in the exponential and stationary phases of growth, respectively (3, 9). However, an explanation for this phenomenon had been missing ever since.

To determine whether amyloid was related to this sudden loss of Mcc activity, the *in vivo* formation of amyloid was evaluated by PK digestion (Fig. 5*B*), sedimentation assay (Fig. 5*C*), and electron microscopy (Fig. 6). Fig. 5*B* shows an immunoblot of culture samples treated or not with PK. Although the total amount of Mcc was found to gradually increase during cell growth, almost no PK-resistant Mcc could be detected up to 9 h

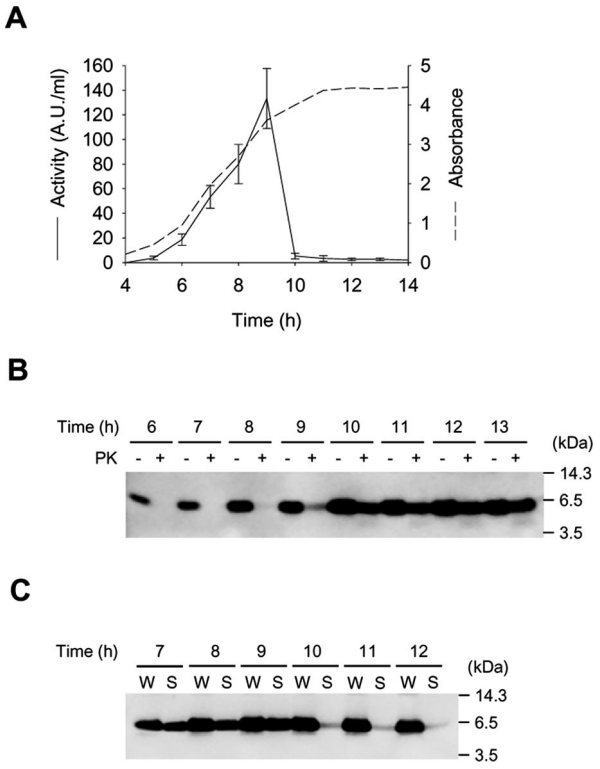

FIG. 5. **Mcc activity *in vivo* is modulated by protein aggregation.** *A*, *E. coli* BL21pJEM15 was grown in culture medium. Mcc activity was measured in the medium by the critical dilution method (*solid line*), and cell growth was followed by recording the absorbance of the culture at 600 nm (*dashed line*) at the indicated times. Note the different scale for each line. *B*, immunoblot of aliquots taken from the culture used in *panel A* at the indicated times that were digested (+) or not (−) with PK (3 μg/ml). *C*, immunoblot of aliquots taken from the culture used in *panel A* at the indicated times that were either directly analyzed (*W,* whole) or previously rid of insoluble material by centrifugation at 16,000 × *g* for 5 min at room temperature (*S,* supernatant).

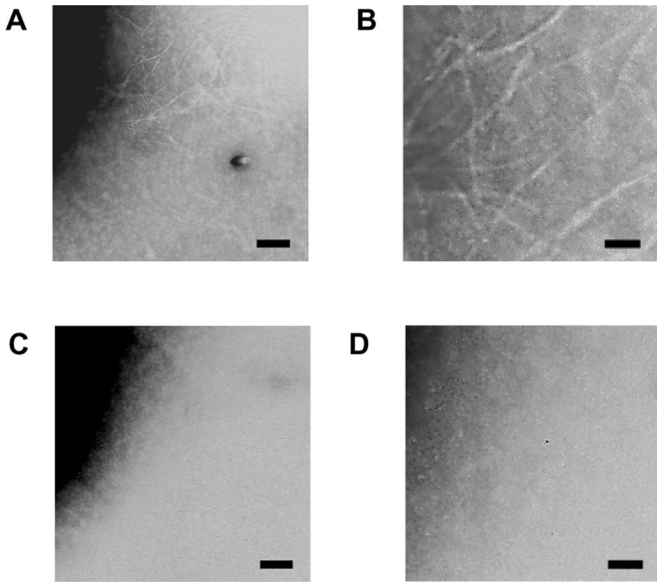

FIG. 6. ***In vivo* amyloid fibril formation in bacterial cultures expressing Mcc.** *E. coli* BL21pJEM15 was grown for 15 h in culture medium and examined using a magnification of ×15,000 (*A*) and ×40,000 (*B*). *E. coli* BL21np108, used as a control strain that does not secrete Mcc, was grown for 15 h and examined using a magnification of ×15,000 (*C*) and ×40,000 (*D*). For these experiments 5 μl of total bacterial culture (cells plus medium) were loaded onto electron microscope grids and stained as described under "Experimental Procedures." The *dark areas* in the upper left corners of *panels A* and *C* correspond to bacterial cells. *Bars*, 200 nm (*A* and *C*) and 50 nm (*B* and *D*).

of culture. Strikingly, a strong PK resistance was observed after 10 h and was maintained in subsequent time points, which coincides with the reported loss of activity. In agreement with our *in vitro* data showing a negative correlation between Mcc activity and resistance to PK digestion (Fig. 4), these *in vivo* results suggest that the formation of amyloid also occurs in a bacterial culture and that it profoundly affects the activity of the protein.

To further study the relationship between Mcc aggregation and activity, we performed sedimentation assays on culture samples to analyze the amount of soluble and aggregated protein at each time, as described under "Experimental Procedures." The results show that although most Mcc appeared to be soluble up to 9 h, virtually no soluble protein could be detected at 10 h and later (Fig. 5*C*). These results are in agreement with what was observed *in vitro*, where Mcc was found to become rapidly insoluble after several hours of incubation (Fig. 3*C*). This finding is again in accordance with the proposition that amyloid formation is responsible for the reported loss of Mcc activity.

Finally, to confirm that amyloid-like fibrils were indeed formed *in vivo*, samples of *E. coli* BL21pJEM15 culture grown for 15 h were analyzed by electron microscopy. Amyloid-like fibrils resembling those obtained *in vitro* were observed (Fig. 6, *A* and *B*), whereas no such structures could be detected in samples of *E. coli* BL21np108 (a mutant that does not export Mcc) (27) culture grown for 15 h (Fig. 6, *C* and *D*). In addition, no fibrils could be observed in samples of *E. coli* BL21pJEM15 culture grown for 8 h only (data not shown), which is consistent with the finding that Mcc is soluble and sensitive to PK digestion at this time point (Fig. 5).

DISCUSSION

The misfolding, aggregation, and tissue accumulation of proteins into fibrillar amyloid deposits is a hallmark process in a variety of neurological and systemic disorders, collectively called protein misfolding diseases (11–13, 18). Compelling evidence indicates that the formation of β-sheet-rich oligomeric and fibrillar structures is the triggering factor in these diseases, which comprise more than 20 different disorders, including Alzheimer, Parkinson, and prion diseases as well as diabetes type 2. These findings have led to the notion that amyloid formation is an inherently negative process implicated in pathological conditions in complex organisms. Here we have shown that amyloid formation also occurs in prokaryotes and is involved in modulating the biological activity of Mcc. Strikingly, the biochemical, structural, morphological, and tinctorial properties of the Mcc aggregates are identical to those observed in the disease protein accumulations. In addition, the mechanism of amyloid formation following a seeding-nucleation polymerization process and the formation of cytotoxic oligomeric structures are also hallmark properties of protein aggregation in the disease conditions. Therefore, amyloidogenesis cannot be considered as a process associated exclusively with diseases in higher organisms but should rather be viewed as a conserved mechanism to control the biological function of diverse proteins.

The mode of action of Mcc has been shown to involve the formation of ion-permeable pores in the cytoplasmic membrane of target bacteria. Indeed, purified Mcc was found to depolarize and permeabilize the *E. coli* cytoplasmic membrane (5, 6) and to form ion channels in phospholipids bilayers *in vitro* (7). Interestingly, Mcc is not only active against bacteria but was also found to cause apoptosis and necrosis in some eukaryotic cell lines (29). The finding that Mcc is able to induce cell death and aggregate into amyloid fibrils is particularly intriguing and could offer a good model by which to study the mechanism of cytotoxicity of disease-causing misfolded protein aggregates.

Strikingly, the emerging notion in protein misfolding diseases is that the toxic species might be oligomeric pore-like structures that may cause cell damage by altering ionic homeostasis (30). Indeed, ordered prefibrillar oligomeric pores have been proposed to be responsible for cell death in Alzheimer and Parkinson diseases (31, 32). A similar phenomenon has been proposed to be involved in diabetes type 2, as protofibrillar islet amyloid polypeptide was found to permeabilize synthetic vesicles by a pore-like mechanism (33). Interestingly, small annular Aβ and α-synuclein protofibrils were reported to resemble the cytolytic β-barrel pore-forming toxins from bacteria such as *Clostridium perfringens* (32, 34), suggesting that a common structure could be responsible for toxic membrane permeabilization. However, the formation of amyloid-like fibrils made of bacterial toxins had not been reported until now, and this parallel was only based on a shared pore-like structure. The oligomerization states of the soluble secreted Mcc and of the toxic pore structures that are formed in target membranes, as well as their relations with the oligomeric intermediates that are present during the amyloid formation process, are currently under investigation in our laboratory.

The finding that Mcc aggregation into amyloid fibrils is associated with a loss of toxicity against target bacteria supports the view that mature amyloid fibrils accumulating in amyloidoses may not be toxic but rather may be considered as inert end products or even as a protective mechanism to sequester the toxic intermediates (30).

Whether Mcc amyloid formation *in vivo* is a regulated process possibly involving post-translational modifications or interactions with other proteins is an intriguing issue that still needs to be addressed. Mcc activity has been reported to be increased under certain growth conditions by the post-translational covalent linkage to its C terminus of a glucose moiety linked to a trimer of 2,3-dihydroxybenzoylserine (35). Although the mechanism by which post-translationally modified Mcc is more active than its non-modified counterpart remains unclear, one possibility would be that this modification stabilizes toxic oligomeric structures and/or prevents the formation of harmless mature amyloid fibrils. Indeed, it has been extensively reported that a variety of post-translational modifications could alter the ability of disease-associated amyloid proteins to aggregate into amyloid fibrils (36). Specific proteins and other compounds have also been shown to promote or inhibit amyloid formation by various proteins (37). Interestingly, enterochelin, a trilactone siderophore that is naturally produced by Enterobacteriaceae, has been reported to inhibit the activity of Mcc (38). Whether this effect is related or not with amyloid formation remains to be determined.

Our findings with Mcc show that protein aggregation into amyloid fibrils might be a generic property of proteins not necessarily associated to a pathological condition. Cytotoxicity may be determined by common features of specific types of aggregates rather than by the primary structure of the proteins involved (39). However, in contrast with amyloidoses where the protein aggregates accumulate in an uncontrolled manner, in the case of Mcc, bacteria use these properties to kill target cells as part of a normal physiological process that confers them competitive advantage. Amyloid formation was previously reported in bacteria when fibers produced by *E. coli* called curli were shown to consist of amyloid fibrils (40). However, unlike Mcc, curli fibers are not involved in cellular toxicity but seem to have structural functions related to the colonization of inert surfaces and biofilm formation. The involvement of amyloid in regulating the biological activity of a bacterial protein suggests that formation of these fibrillar aggregates is an evolutionarily conserved property of proteins that is not only implicated in pathological conditions but also might be used for specific physiological functions.

Acknowledgments—We thank Claudio Hetz, Céline Adessi, June Yowtak, and Octavio Monasterio for helpful discussions and technical advice.

REFERENCES

1. Riley, M. A. (1998) *Annu. Rev. Genet.* **32,** 255–278
2. Riley, M. A., Goldstone, C. M., Wertz, J. E., and Gordon, D. (2003) *J. Evol. Biol.* **16,** 690–697
3. de Lorenzo, V., Martinez, J. L., and Asensio, C. (1984) *J. Gen. Microbiol.* **130,** 391–400
4. de Lorenzo, V. (1984) *Arch. Microbiol.* **139,** 72–75
5. Destoumieux-Garzon, D., Thomas, X., Santamaria, M., Goulard, C., Barthelemy, M., Boscher, B., Bessin, Y., Molle, G., Pons, A. M., Letellier, L., Peduzzi, J., and Rebuffat, S. (2003) *Mol. Microbiol.* **49,** 1031–1041
6. de Lorenzo, V., and Pugsley, A. P. (1985) *Antimicrob. Agents Chemother.* **27,** 666–669
7. Lagos, R., Wilkens, M., Vergara, C., Cecchi, X., and Monasterio, O. (1993) *FEBS Lett.* **321,** 145–148
8. Baquero, F., and Moreno, F. (1984) *FEMS Microbiol. Lett.* **23,** 117–124
9. de Lorenzo, V. (1985) *J. Antibiot.* **38,** 340–345
10. Corsini, G., Baeza, M., Monasterio, O., and Lagos, R. (2002) *Biochimie (Paris)* **84,** 539–544
11. Soto, C. (2001) *FEBS Lett.* **498,** 204–207
12. Dobson, C. M. (1999) *Trends Biochem. Sci.* **24,** 329–332
13. Carrell, R. W., and Lomas, D. A. (1997) *Lancet* **350,** 134–138
14. Miller, J. H. (1972) *Experiments in Molecular Genetics*, pp. 431–435, Cold Spring Harbor Laboratory, Cold Spring Harbor, New York
15. Pons, A. M., Zorn, N., Vignon, D., Delalande, F., Van Dorsselaer, A., and Cottenceau, G. (2002) *Antimicrob. Agents Chemother.* **46,** 229–230
16. Mayr-Harting, A., Hedges, A. J., and Berkeley, R. C. W. (1972) in *Methods in Microbiology* (Norris, J. R., and Ribbons, D. N., eds) Vol. 7A, pp. 315–422, Academic Press, New York
17. Sunde, M., and Blake, C. (1997) *Adv. Protein Chem.* **50,** 123–159
18. Soto, C. (2003) *Nat. Rev. Neurosci.* **4,** 49–60
19. Glenner, G. G. (1980) *N. Engl. J. Med.* **302,** 1283–1292
20. Sipe, J. D., and Cohen, A. S. (2000) *J. Struct. Biol.* **130,** 88–98
21. Klunk, W. E., Jacob, R. F., and Mason, R. P. (1999) *Methods Enzymol.* **309,** 285–305
22. LeVine, H., III (1999) *Methods Enzymol.* **309,** 274–284
23. Bolton, D. C., McKinley, M. P., and Prusiner, S. B. (1982) *Science* **218,** 1309–1311
24. Nordstedt, C., Naslund, J., Tjernberg, L. O., Karlstrom, A. R., Thyberg, J., and Terenius, L. (1994) *J. Biol. Chem.* **269,** 30773–30776
25. Harper, J. D., and Lansbury, P. T., Jr. (1997) *Annu. Rev. Biochem.* **66,** 385–407
26. Saborio, G. P., Permanne, B., and Soto, C. (2001) *Nature* **411,** 810–813
27. Lagos, R., Baeza, M., Corsini, G., Hetz, C., Strahsburger, E., Castillo, J. A., Vergara, C., and Monasterio, O. (2001) *Mol. Microbiol.* **42,** 229–243
28. Wilkens, M., Villanueva, J. E., Cofre, J., Chnaiderman, J., and Lagos, R. (1997) *J. Bacteriol.* **179,** 4789–4794
29. Hetz, C., Bono, M. R., Barros, L. F., and Lagos, R. (2002) *Proc. Natl. Acad. Sci. U. S. A.* **99,** 2696–2701
30. Caughey, B., and Lansbury, P. T. (2003) *Annu. Rev. Neurosci.* **26,** 267–298
31. Lashuel, H. A., Petre, B. M., Wall, J., Simon, M., Nowak, R. J., Walz, T., and Lansbury, P. T. (2002) *J. Mol. Biol.* **322,** 1089–1102
32. Lashuel, H. A., Hartley, D., Petre, B. M., Walz, T., and Lansbury, P. T. (2002) *Nature* **418,** 291
33. Anguiano, M., Nowak, R. J., and Lansbury, P. T., Jr. (2002) *Biochemistry* **41,** 11338–11343
34. Hotze, E. M., Heuck, A. P., Czajkowsky, D. M., Shao, Z. F., Johnson, A. E., and Tweten, R. K. (2002) *J. Biol. Chem.* **277,** 11597–11605
35. Thomas, X., Destoumieux-Garzon, D., Peduzzi, J., Afonso, C., Blond, A., Birlirakis, N., Goulard, C., Dubost, L., Thai, R., Tabet, J. C., and Rebuffat, S. (2004) *J. Biol. Chem.* **279,** 28233–28242
36. Atwood, C. S., Martins, R. N., Smith, M. A., and Perry, G. (2002) *Peptides* **23,** 1343–1350
37. Soto, C. (1999) *Mol. Med. Today* **5,** 343–350
38. Orellana, C., and Lagos, R. (1996) *FEMS Microbiol. Lett.* **136,** 297–303
39. Bucciantini, M., Giannoni, E., Chiti, F., Baroni, F., Formigli, L., Zurdo, J. S., Taddei, N., Ramponi, G., Dobson, C. M., and Stefani, M. (2002) *Nature* **416,** 507–511
40. Chapman, M. R., Robinson, L. S., Pinkner, J. S., Roth, R., Heuser, J., Hammar, M., Normark, S., and Hultgren, S. J. (2002) *Science* **295,** 851–855